# Chemical Communications

## COMMUNICATION

# Dy-carboxylate nanomeshes with tunable cavity size and assembly motif through ionic interactions

B. Cirera,[a] L. Đorđević,[b] R. Otero,[a,c] J. M. Gallego,[d] D. Bonifazi,[b,e,*], R. Miranda[a,c] and D. Ecija[a,*]

**We report the design of dysprosium directed metallo-supramolecular architectures on a pristine Cu(111) surface. By an appropiate selection of the ditopic molecular linkers equipped with terminal carboxylic groups (TPA, PDA and TDA species), we create reticular and mononuclear metal-organic nanomeshes of tunable internodal distance, which are stabilized by eight-fold Dy···O interactions. A thermal annealing treatment for the reticular Dy:TDA architecture gives rise to an unprecedented quasi-hexagonal nanostructure based on dinuclear Dy clusters, exhibiting a unique six-fold Dy···O bonding motif. All metallo-supramolecular architectures are stable at room temperature. Our results open new avenues for the engineering of supramolecular architectures on surfaces incorporating f-block elements forming thermally robust nanoarchitectures through ionic bonds.**

Coordination chemistry on surfaces has emerged as a powerful strategy to design on-surface confined functional materials with prospects in sensing, catalysis, molecular electronics and magnetism.[1-5] To this aim, molecular species conveniently equipped with pyridyl, terpyridyl, carbonitrile and carboxylate terminal moieties have been shown to coordinate with distinct metals including d-block and alkali elements giving rise to a large variety of supramolecular structures, ranging from discrete entities to monodimensional and bidimensional architectures.[6-21] Of a particular interest, it has been the quest for deterministic engineering of metallo-supramolecular architectures, which revealed great success for carboxylate and carbonitrile functional groups coordinating d-block elements.

Surprisingly, despite the use of rare-earths in high technology,[22-25] coordination chemistry of lanthanides on surfaces has been only recently tackled on coinage metals.[26-30] Specifically, we have showed that carboxylate moieties could be exploited to design a thermally robust gadolinium-driven reticular architecture, in which the nature of the bond indicated ionic characteristics.[29] It is of timely relevance to engineer metallo-supramolecular architectures based on predominant ionic interactions in a deterministic way, enhancing the scope for supramolecular design of metal-organic interactions on surfaces, while simultaneously incorporating the functionalities of the f-block elements.

Here we report a scanning ~~tunneling~~tunnelling microscopy study, complemented with X-ray photoelectron spectroscopy, of Dy-directed metallo-supramolecular assemblies on pristine Cu(111) involving ditopic linkers equipped with terminal carboxylic moieties and with molecular backbones of *ex-professo* distinct spacing lengths. In particular, we focus on *p*-terphenyl-4,4''-dicarboxylic acid (TDA), pyrene-2,7-dicarboxylic acid (PDA) and benzene-1,4-dicarboxylic acid (TPA) molecular modules (*cf.* Figure S1). Our results show that, after deprotonation of the molecular precursors, reticular architectures displaying different sizes could be prepared through Dy atoms engaged in an eight-fold Dy-O coordination interactions. Furthermore, the grid afforded by Dy-driven deprotonated TDA precursors could be thermally converted into a quasi-hexagonal network based on dinuclear Dy clusters. The spectroscopic characteristics of the bonds suggest a strong ionic nature. Notably, all metallo-supramolecular architectures are stable at room temperature.

The deposition of TDA species on Cu(111) held at 373 K to promote full deprotonation of the carboxylate functional groups[29] followed by sublimation of dysprosium allows the formation of reticular assemblies, where the molecular species are imaged as bright dots, and the dysprosium mononuclear centers as voids (*cf.* Figure 1a) or dim protrusions (*cf.* Figure S2) depending on tip condition.

[a] IMDEA Nanoscience, 28049 Madrid, Spain. E-mail: david.ecija@imdea.org
[b] Department of Pharmaceutical and Chemical Sciences and INSTM UdR Trieste; University of Trieste; Piazzale Europa 1, Trieste 34127, Italy
[c] Departamento Física de la Materia Condensada, Universidad Autónoma de Madrid, 28049 Madrid, Spain
[d] Instituto de Ciencia de Materiales de Madrid, CSIC, 28049 Madrid, Spain
[e] School of Chemistry, Cardiff University, Main Building, Park Place, Cardiff CF10 3AT, United Kingdom; Email: bonifazid@cardiff.ac.uk

An atomistic model displayed in Figure 2b reveals that the stability of the architecture is based on an eight-fold Dy-oxygen coordination motif with an internodal projected distance of 20.5 ± 0.5 Å, resulting in an average distance Dy···O of 2.4 ± 0.5 Å. This is very similar to that observed in Gd-directed assemblies.[29] Further annealing to 450 K induces a phase-transition giving rise to a new metallo-supramolecular architecture that can be rationalized as a quasi-hexagonal network in which the dinuclear Dy ~~centers~~centres are distanced by 5.8 Å (*cf.* Figure 1c). The atomistic model reveals a unique coordination motif, whereby each Dy ~~center~~centre is engaged in six Dy···O coordination bonds, and in which four molecules are connected to one single dysprosium and the two additional linkers are sharing the two Dy atoms. The dinuclear nodes can present three distinct orientations with respect to the substrate, being their irregular distribution on the surface dictated by a subtle combination between metal-organic coordination and interactions with the substrate. Most of the molecular species align with the close-packed directions of the surface. However, triggered by steric repulsion, there is always some misalignment giving rise to the final appearance of a distorted supramolecular hexagonal architecture.
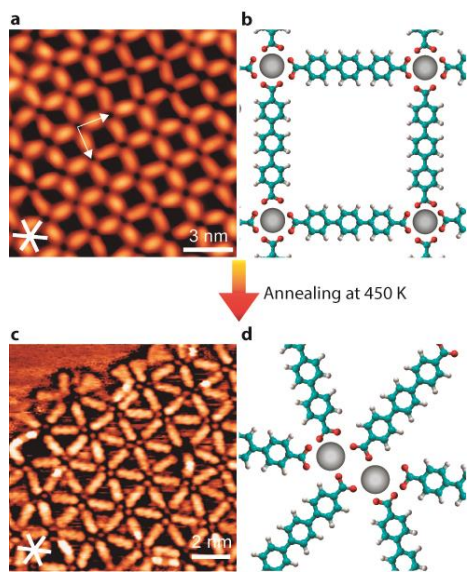


**Figure 1. Lanthanide-directed Dy:TDA metallo-supramolecular networks on Cu(111) upon thermal annealing.** (a-b) Dy:TDA reticular mononuclear architecture achieved by depositing TDA and Dy on a surface held at 373 K. (a) High resolution STM image ($V_b$ = -0.8 V and I = 150 pA). White arrows indicate the lattice vectors of the porous network with a length of ~ 20.5 ± 0.5 Å. Image recorded at 4 K. (b) Atomistic model of a, indicating an eight-fold Dy···O coordination motif. (c-d) Dy:TDA quasi-hexagonal dinuclear network obtained by annealing (a) to 450 K. (c) High resolution STM Image ($V_b$ = -1.2 V and I = 320 pA), showing the quasi-hexagonal porous network with internodal distances in the range from 19 to 23.5 ± 0.5 Å. Image recorded at room temperature. (d) Atomistic model of (c) indicating a six-fold Dy···O coordination.

To further shed light on the chemical properties of the molecular and lanthanides species along with the nature of the Dy···O metal-organic bonds, all Dy-directed supramolecular architectures have been inspected by in-situ X-ray photoelectron spectroscopy.
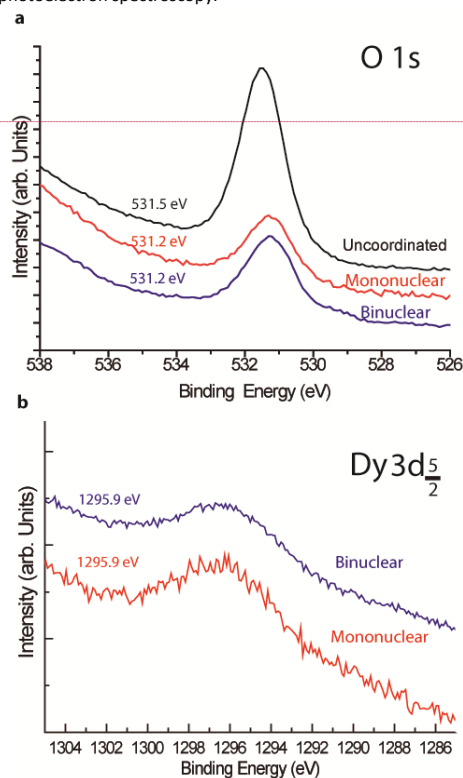


**Figure 2. X-ray photoemission spectroscopy of Dy:TDA architectures on Cu(111).** (a) XPS spectra of the O1s core level for the uncoordinated species (deprotonated), mononuclear and binuclear architectures (cf. Figures 1a,b and 1c,d for structural details, respectively). (b) Dy $3d_{5/2}$ spectra for the binuclear and the mononuclear networks.

In Figure 2a, the O 1s XPS data is shown for a TDA submonolayer deposited on the Cu surface held at room temperature and annealed up to 373 K (upper black curve), a TDA submonolayer after co-adsorption of Dy at a surface temperature of 373 K (middle red curve), and a TDA submonolayer after coadsorption of Dy at a surface temperature of 473 K (bottom violet curve). The TDA submonolayer only presents a peak at 531.5 eV, which is associated with two chemically identical oxygen atoms in the carboxylate moieties,[31, 32] deriving from the full deprotonation of the TDA species on Cu(111) at 373 K.[29] Upon deposition of Dy atoms on the sample at 373 K, the peak shifts 0.3 eV to a lower binding energy of 531.2 eV. Further annealing of the

COMMUNICATION

sample to 450 K results in negligible changes, despite the significant structural change reported above (*cf.* Figure 1a-d). Figure 2b presents the Dy 3d$_{5/2}$ XPS spectra for the Dy-TDA supramolecular architectures (same experiments as that addressed in Figure 2a). The spectra show broad peak for both samples (with a peak width typical of lanthanide systems) at 1295.9 eV. A comparison to literature data reveals that the binding energy of the Dy 3d$_{5/2}$ peak is in excellent agreement with Dy in a +3 oxidation state (1296 eV).[33]

These results are similar to those recently reported for Cs-BPyDA[32] and Na-TPA[18] supramolecular architectures on Cu(100) surfaces and for Gd-carboxylate reticular networks,[29] in which a predominant ionic character of the metal-organic bond is proposed. This strongly differs from the metal-organic bond in Fe-carboxylate architectures,[31, 34] where a prevalent covalent nature has been suggested.[32]

Next, in order to modulate the inter-lanthanide distance of the reticular phase, we have studied the coordination of PDA and TPA modules with Dy atoms in independent experiments.
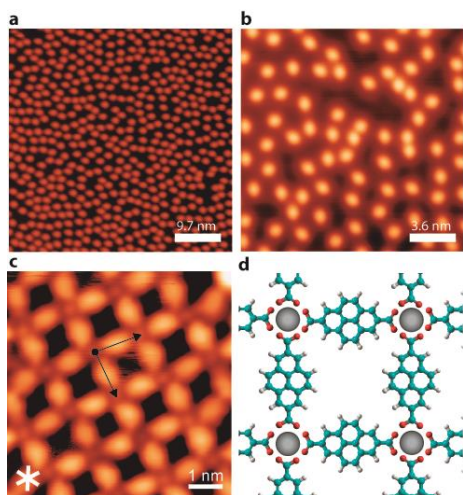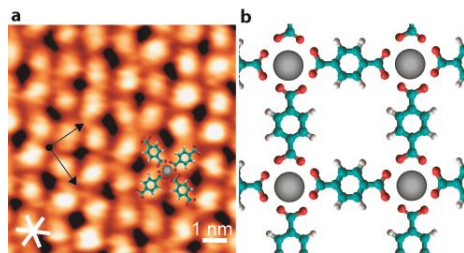


**Figure 3. Lanthanide-directed Dy:PDA metallo-supramolecular network on Cu(111).** (a) Long range STM image of deprotonated PDA species. (V$_b$ = 1 V and I = 80 pA). (b) Zoom-in image highlighting isolated species. (V$_b$ = -1 V and I = 100 pA). (c) High resolution STM image of the Dy-directed architecture (V$_b$ = 2.5 V and I = 50 pA). The black arrows indicate the square porous network with a lattice vector of ~ 15.0 ± 0.5 Å, whereas the white cross displays the close-packed directions of the surface. (d) Tentative atomistic model of (c). Images recorded at 4 K.

The sublimation of the synthesized PDA species (cf. Supporting Information for the synthetic procedures) on Cu(111) held at 373 K to achieve full deprotonation results in a random distribution of individual molecular species, which are imaged as bright rods (*cf.* Fig. 3a-b). After the deposition of Dy atoms with the sample at 373 K, the appearance of a porous metallo-supramolecular grid clearly emerges, where the pyrene

molecular backbones are visualized as bright rectangular rods and the Dy atoms are imaged as dim protrusions. Importantly, one of the linear directions of the reticular grid is aligned with the close-packed directions of the substrate. The corresponding atomistic model reveals that the metal-organic network is stabilized by eight-fold Dy···O coordination interactions, like in the TDA network shown in Figures 1a-b. The average projected internodal distance is of 15.4 ± 0.5 Å, thus resulting in an average projected Dy···O bond length of 2.4 ± 0.5 Å.

Figure 4 displays the smallest lanthanide-directed porous metallo-supramolecular network created by the deposition of TPA species on Cu(111), held at 100°C373 K to favour deprotonation,[31, 35, 36] and Dy. Fully deprotonated molecular species are visualized as bright lobes, whereas the lanthanide centerscentres are imaged as voids. Like in former cases, there is an alignment of one of the network lattice vectors with the close-packed directions of the surface. The stability of the metallo-supramolecular architecture is provided by eight-fold Dy···O coordination motifs, with a Dy-Dy projected internodal distance of 12.8 ± 0.5 Å, resulting in an average projected Dy···O bond length of 2.4 ± 0.5 Å.



**Figure 4. Smallest porous lanthanide-directed metallo-supramolecular architecture formed by depositing TPA and Dy on Cu(111).** (a) (a) High resolution STM image (V$_b$ = 1.1 V and I = 150 pA). Black arrows indicate the square porous network with a lattice vector of 12.8 ± 0.5 Å. White cross displays close-packed directions of the surface. Image recorded at room temperature. (b) Tentative atomistic model of (a).

Thanks to the ionic character of the bonds and the molecule-substrate interaction, all reported metallo-supramolecular architectures exhibit certain degree of flexibility showing some molecular species slightly misaligned.

Under appropriate growth conditions and within the submonolayer regime, domains spanning tens of nanometersnanometres for the metallo-supramolecular architectures could be achieved (*cf.* Supporting Information).

Importantly, we explored the evolution of the dysprosium directed DPA and TPA reticular architectures upon thermal annealing without the detection of a single six-fold Dy···O coordinative motif, thus revealing a different phase behaviorbehaviour than in the TDA case. This result suggests a very subtle balance between dysprosium diffusion, molecular diffusion, molecular steric hindrance due to distinct backbone lengths and molecule-substrate interaction, which allows the expression of six-fold Dy···O coordinative motifs for TDA

provided sufficient thermal annealing, but blocks the presence of such a bond for the DPA an TPA cases.

In summary, we have reported a scanning ~~tunneling~~tunnelling microscopy study of Dy-directed porous metallo-supramolecular architectures on Cu(111) based on the coordination of carboxylate moieties with Dy ~~centers~~centres. By a careful selection of the backbone length of conveniently equipped ditopic linkers, the tuning of the internodal distance (from 11 Å to 19 Å) of reticular metal-organic networks could be achieved. Furthermore, a thermal treatment of the reticular Dy:TDA assemblies resulted in a quasi-hexagonal porous architecture based on unprecedented dinuclear Dy vertexes, in which a unique coordination motif between two metallic atoms and twelve surrounding O atoms was found. These findings will certainly open new avenues for the design of surface-confined multinuclear metal-organic architectures of great relevance in fundamental and applied science to elucidate metal-metal, metal-ligand and metal-adsorbates interactions and resulting properties. Importantly, our microscopy data were complemented by X-ray photoelectron spectroscopy, which in accordance with literature data, suggests a strong ionic contribution of the Dy···O bond, as normally encountered in lanthanide-based coordinative architectures. Thus, our results reveal the feasibility of tuning surface-confined metallo-supramolecular architectures on surfaces based on ionic interactions, while potentially incorporating the functionalities of the f-block family.

## Notes and references

For experimental methods and modelling see Supporting Information.

1. J. V. Barth, G. Costantini and K. Kern, *Nature*, 2005, **437**, 671-679.
2. J. V. Barth, *Annu. Rev. Phys. Chem.*, 2007, **58**, 375-407.
3. J. V. Barth, *Surf. Sci.*, 2009, **603**, 1533-1541.
4. L. Bartels, *Nat. Chem.*, 2010, **2**, 87-95.
5. D. Bonifazi, S. Mohnani and A. Llanes-Pallas, *Chem. Eur. J.*, 2009, **15**, 7004-7025.
6. N. Lin, A. Dmitriev, J. Weckesser, J. V. Barth and K. Kern, *Angew. Chem. Int. Ed.*, 2002, **41**, 4779-4783.
7. P. Messina, A. Dmitriev, N. Lin, H. Spillmann, M. Abel, J. V. Barth and K. Kern, *J. Am. Chem. Soc.*, 2002, **124**, 14000-14001.
8. A. Dmitriev, H. Spillmann, N. Lin, J. V. Barth and K. Kern, *Angew. Chem. Int. Ed.*, 2003, **41**, 2670 - 2673.
9. S. Stepanow, M. Lingenfelder, A. Dmitriev, H. Spillmann, E. Delvigne, N. Lin, X. Deng, C. Cai, J. V. Barth and K. Kern, *Nat. Mater.*, 2004, **3**, 229-233.
10. S. Stepanow, N. Lin, F. Vidal, A. Landa, M. Ruben, J. V. Barth and K. Kern, *Nano Lett.*, 2005, **5**, 901-904.
11. W. Auwärter, F. Klappenberger, A. Weber-Bargioni, A. Schiffrin, T. Strunskus, C. Wöll, Y. Pennec, A. Riemann and J. V. Barth, *J. Am. Chem. Soc.*, 2007, **129**, 11279-11285.
12. U. Schlickum, R. Decker, F. Klappenberger, G. Zopellaro, S. Klyatskaya, M. Ruben, I. Silanes, A. Arnau, K. Kern, H. Brune and J. V. Barth, *Nano Lett.*, 2007, **7**, 3813-3817.
13. D. Ecija, M. Trelka, C. Urban, P. d. Mendoza, E. Mateo-Martín, C. Rogero, J. A. Martín-Gago, A. M. Echavarren, R. Otero, J. M. Gallego and R. Miranda, *J. Phys. Chem. C*, 2008, **112**, 8988-8994.
14. T. Tseng, C. Urban, Y. Wang, R. Otero, S. L. Tait, M. Alcami, D. Ecija, M. Trelka, J. M. Gallego, N. Lin, M. Konuma, U. Starke, A. Nefedov, A. Langner, C. Wöll, M. A. Herranz, F. Martin, N. Martin, K. Kern and R. Miranda, *Nat. Chem.*, 2009, **2**, 374-379.
15. D. Heim, D. Ecija, K. Seufert, W. Auwärter, C. Aurisicchio, C. Fabbro, D. Bonifazi and J. V. Barth, *J. Am. Chem. Soc.*, 2010, **132**, 6783-6790.
16. D. Ecija, S. Vijayaraghavan, W. Auwärter, S. Joshi, K. Seufert, C. Aurisicchio, D. Bonifazi and J. V. Barth, *ACS Nano*, 2012, **6**, 4258-4265.
17. Y. Li, J. Xiao, T. E. Shubina, M. Chen, Z. Shi, M. Schmid, H.-P. Steinrück, J. M. Gottfried and N. Lin, *J. Am. Chem. Soc.*, 2012, **134**, 6401-6408.
18. D. Skomski, S. Abb and S. L. Tait, *J. Am. Chem. Soc.*, 2012, **134**, 14165-14171.
19. N. Abdurakhmanova, A. Floris, T.-C. Tseng, A. Comisso, S. Stepanow, A. De Vita and K. Kern, *Nat. Commun.*, 2012, **3**, 940.
20. C. S. Kley, J. Čechal, T. Kumagai, F. Schramm, M. Ruben, S. Stepanow and K. Kern, *J. Am. Chem. Soc.*, 2012, **134**, 6072-6075.
21. L. Fendt, M. Stöhr, N. Wintjes, M. Enache, T. A. Jung and F. Diederich, *Chem. Eur. J.*, 2009, **15**, 11139-11150.
22. J.-C. G. Bünzli, *Acc. Chem. Res.*, 2006, **39**, 53-61.
23. S. V. Eliseeva and J.-C. G. Bunzli, *Chem. Soc. Rev.*, 2010, **39**, 189-227.
24. S. V. Eliseeva and J.-C. G. Bünzli, *New J. Chem.*, 2011, **35**, 1165-1176.
25. J.-C. G. Bünzli, *J. Coord. Chem.*, 2014, **67**, 3706-3733.
26. D. Écija, J. I. Urgel, A. C. Papageorgiou, S. Joshi, W. Auwärter, A. P. Seitsonen, S. Klyatskaya, M. Ruben, S. Fischer, S. Vijayaraghavan, J. Reichert and J. V. Barth, *Proc. Natl. Acad. Sci. USA.*, 2013, **110**, 6678-6681.
27. J. I. Urgel, D. Ecija, W. Auwärter and J. V. Barth, *Nano Lett.*, 2014, **14**, 1369.
28. J. I. Urgel, D. Ecija, W. Auwärter, A. C. Papageorgiou, A. P. Seitsonen, S. Vijayaraghavan, S. Joshi, S. Fischer, J. Reichert and J. V. Barth, *J. Phys. Chem. C*, 2014, **118**, 12908-12915.
29. J. I. Urgel, B. Cirera, Y. Wang, W. Auwärter, R. Otero, J. M. Gallego, M. Alcamí, S. Klyatskaya, M. Ruben, F. Martin, N. Miranda, D. Ecija and J. V. Barth, *Small*, 2015, **47**, 6358-6364.
30. J. I. Urgel, D. Ecija, W. Auwärter, D. Stassen, D. Bonifazi and J. V. Barth, *Angew. Chem. Int. Ed.*, 2015, **54**, 6163-6167.
31. S. Stepanow, T. Strunskus, M. Lingenfelder, A. Dmitriev, H. Spillmann, N. Lin, J. V. Barth, C. Wöll and K. Kern, *J. Phys. Chem. B*, 2004, **108**, 19392-19397.
32. S. Stepanow, R. Ohmann, F. Leroy, N. Lin, T. Strunskus, C. Woll and K. Kern, *Acs Nano*, 2010, **4**, 1813-1820.
33. Y. A. Teterin and A. Yu. Teterin, *Russian Chemical Reviews*, 2002, **71**, 347-381.
34. S. L. Tait, Y. Wang, G. Costantini, N. Lin, A. Baraldi, F. Esch, L. Petaccia, S. Lizzit and K. Kern, *J. Am. Chem. Soc.*, 2008, **130**, 2108-2113.
35. T. Schmitt, L. Hammer and M. A. Schneider, *The Journal of Physical Chemistry C*, 2016, **120**, 1043-1048.
36. T. W. White, University of Warwick, 2014.